

Strange hadronic loops of the proton: A quark model calculation

Paul Geiger

Department of Physics, Carnegie Mellon University, Pittsburgh, Pennsylvania 15213

Nathan Isgur

Jefferson Lab, 12 000 Jefferson Avenue, Newport News, Virginia 23606

(Received 13 May 1996)

Nontrivial $q\bar{q}$ sea effects have their origin in the low- Q^2 dynamics of strong QCD. We present here a quark model calculation of the contribution of $s\bar{s}$ pairs arising from a *complete* set of OZI-allowed strong Y^*K^* hadronic loops to the net spin of the proton, to its charge radius, and to its magnetic moment. The calculation is performed in an “unquenched quark model” which has been shown to preserve the spectroscopic successes of the naive quark model and to respect the OZI rule. We speculate that an extension of the calculation to the nonstrange sea will show that most of the “missing spin” of the proton is in orbital angular momenta. [S0556-2821(97)00601-2]

PACS number(s): 14.20.Dh, 12.38.Aw, 12.39.Ba, 13.25.-k

I. INTRODUCTION

While providing a good description of low-energy strong interaction phenomena, the constituent quark model appears to be inconsistent with many fundamental characteristics of QCD. Foremost among these inconsistencies is a “degree of freedom problem”: the quark model declares that the low-energy spectrum of QCD is built from the degrees of freedom of spin- $\frac{1}{2}$ fermions confined to a $q\bar{q}$ or qqq system. Thus, for mesons the quark model predicts, and we seem to observe, a “quarkonium” spectrum. In the baryons it predicts, and we seem to observe, the spectrum of two relative coordinates and three spin- $\frac{1}{2}$ degrees of freedom.

These quark model degrees of freedom are to be contrasted with the most naive interpretation of QCD which would lead us to expect a low-energy spectrum exhibiting 36 quark and antiquark degrees of freedom (3 flavors \times 2 spins \times 3 colors for particle and antiparticle), and 16 gluon degrees of freedom (2 spins \times 8 colors). Less naive pictures exist, but none evade the first major “degree of freedom problem” that the gluonic degrees of freedom appear to be missing from the low-energy spectrum. This issue, being one of the most critical in nonperturbative QCD, is being addressed by many theoretical and experimental programs.

The second major “degree of freedom problem,” and the one which we address here, has to do with $q\bar{q}$ pair creation. *A priori*, one would expect pair creation to be so probable that a valence quark model would fail dramatically. Of course, we know empirically that pair creation is suppressed: the observed hadronic spectrum is dominated by narrow resonances, while the naive picture would predict resonances with widths Γ comparable to their masses m .

It is now widely appreciated that the narrow resonance approximation can be rationalized in QCD within the $1/N_c$ expansion [1]: in the limit $N_c \rightarrow \infty$, meson widths (for example) are proportional to N_c^{-1} while their masses are independent of N_c . The demonstration proceeds by showing that hadron two-point functions are dominated by graphs in which the valence quark lines propagate from their point of creation to their point of annihilation without additional

quark loops. The dominance of such a “quenched approximation” is, however, not sufficient to underwrite the valence quark model: in the chiral limit, such Feynman graphs in general receive important contributions from not only forward quark propagation, but also from “Z graphs.” (A “Z graph” is one in which the interactions first produce a pair and then annihilate the antiparticle of the produced pair against the original propagating particle). Cutting through a large N_c two-point function at a fixed time therefore would in general reveal not only the valence quarks but also a large $q\bar{q}$ sea. The large N_c expansion also leaves unanswered a more quantitative question. While hadronic widths Γ are normally small compared to hadronic masses m , they are typically comparable to the mass spacings between states in the hadronic spectrum. It is thus surprising that the spectroscopy of a valence quark model can survive “unquenching.”

There is another puzzle of hadronic dynamics which is reminiscent of this one: the success of the Okubo-Zweig-Iizuka (OZI) rule [2]. A generic OZI-violating amplitude A_{OZI} can also be shown to vanish like $1/N_c$. However, there are several unsatisfactory features of this “solution” to the OZI mixing problem [3]. Consider ω - ϕ mixing as an example. This mixing receives a contribution from the virtual hadronic loop process $\omega \rightarrow K\bar{K} \rightarrow \phi$, both steps of which are OZI allowed, and each of which scales with N_c like $\Gamma^{1/2} \sim N_c^{-1/2}$. The large N_c result that this OZI-violating amplitude behaves like N_c^{-1} is thus not peculiar to large N_c : it just arises from “unitarity” in the sense that the real and imaginary parts of a generic hadronic loop diagram will have the same dependence on N_c . The usual interpretation of the OZI rule in this case, that “double hairpin graphs” are dramatically suppressed, is untenable in the light of these OZI-allowed loop diagrams. They expose the deficiency of the large N_c argument since $A_{\text{OZI}} \sim \Gamma \ll m$ is *not* a good representation of the OZI rule. (Continuing to use ω - ϕ mixing as an example, we note that $m_\omega - m_\phi$ is numerically comparable to a typical hadronic width, so the large N_c result would predict an ω - ϕ mixing angle of order unity in contrast to the observed pattern of very weak mixing which implies that $A_{\text{OZI}} \ll \Gamma \ll m$.)

In our recent papers [4,5], we have studied the unquenching of the quark model, addressing in particular the impact of $q\bar{q}$ pair creation on quark model spectroscopy and on the OZI rule. In this paper we extend our previous work to calculate some effects of the strange quark content of the proton induced by strong $s\bar{s}$ pair creation. Since, as will be described in the next section, our model preserves the spectroscopic successes of the quark model and is consistent with the OZI rule, it provides a legitimate framework for the study of the $q\bar{q}$ sea. We focus here on the $s\bar{s}$ sea both because it allows us to avoid complexities associated with antisymmetrization with respect to the valence quarks in the nucleons, and because it has recently received considerable experimental attention.

Our goals for this calculation, though ambitious, are limited. In particular, we will address here the effects on the strange quark helicity Δs , the strangeness charge radius R_s^2 , and the strangeness magnetic moment μ_s of a complete sum over the OZI-allowed $s\bar{s}$ loops which contribute to two-point functions (i.e., of processes that correspond at the hadronic level to $p \rightarrow Y^* K^* \xrightarrow{j} Y^{*'} K^{*'} \rightarrow p$, where Y^* and K^* represent generic $S = -1$ baryons and $S = +1$ mesons, respectively, and where \xrightarrow{j} indicates the action of the appropriate current). In contrast, we are unable to discuss the effects of pure OZI-forbidden processes (i.e., ones that do not proceed through strong OZI-allowed meson loops). These include processes in which the $s\bar{s}$ pair is directly created or annihilated in a color singlet state (e.g., $p \rightarrow p \phi_{JPC} \xrightarrow{j} p \phi'_{J'P'C'} \rightarrow p$ and $p \xrightarrow{j} p \phi_{JPC} \rightarrow p$ or $p \rightarrow p \phi_{JPC} \xrightarrow{j} p$, where ϕ_{JPC} is an $s\bar{s}$ meson with quantum numbers J^{PC}). The latter two of these processes correspond to pure OZI-forbidden vector-meson-dominance-type graphs. As was the case in our earlier studies of OZI violation [5], all such disconnected ‘‘double-hairpin’’ diagrams are outside of the scope of our model: we focus on the naively much larger OZI-allowed loop diagrams. We also do not discuss here processes in which strange baryon-meson loops are directly created by the probing current. While such ‘‘contact graphs’’ would in general exist, we show below that none are required to make the contributions of our strong $Y^* K^*$ loop graphs to Δs , R_s^2 , or μ_s gauge invariant.

II. UNQUENCHING THE QUARK MODEL: BACKGROUND

The Introduction describes three puzzles associated with the nature and importance of $q\bar{q}$ pairs in low-energy hadron structure: (1) the origin of the apparent valence structure of hadrons (since even as $N_c \rightarrow \infty$, Z graphs would produce pairs unless the quarks were heavy), (2) the apparent absence of unitarity corrections to naive quark model spectroscopy, despite one’s expectation of mass shifts $\Delta m \sim \Gamma$ (where Γ is a typical hadronic width), and (3) the systematic suppression of OZI-violating amplitudes A_{OZI} relative to one’s expectation (from unitarity) that $A_{\text{OZI}} \sim \Gamma$.

In this section we describe the solutions we see to these puzzles. The resulting picture forms the context of the new work described in this paper.

A. The origin of the valence approximation

As already mentioned, a weak form of the valence approximation seems to emerge from the large N_c limit in the sense that diagrams in which only valence quark lines propagate through hadronic two-point functions dominate as $N_c \rightarrow \infty$. This dominance does not seem to correspond to the usual valence approximation since the Z -graph pieces of such diagrams will produce a $q\bar{q}$ sea.

Consider, however, the Dirac equation for a single light quark interacting with a static color source (or a single light quark confined in a bag). This equation represents the sum of a set of Feynman graphs which also include Z graphs, but the effects of those graphs is captured in the lower components of the single particle Dirac spinor. That is, such Z graphs correspond to relativistic corrections to the quark model. That such corrections are important in the quark model has been known for a long time [6]. For us the important point is that while they have quantitative effects on quark model predictions (e.g., they are commonly held to be responsible for much of the required reduction of the nonrelativistic quark model prediction that $g_A = 5/3$ in neutron β decay), they do not qualitatively change the single-particle nature of the spectrum of the quark of our example, nor would they qualitatively change the spectrum of $q\bar{q}$ or qqq systems. Note that this interpretation is consistent with the fact that Z -graph-induced $q\bar{q}$ pairs do *not* correspond to the usual partonic definition of the $q\bar{q}$ sea since Z -graphs vanish in the infinite momentum frame. Thus the $q\bar{q}$ sea of the parton model is also associated with the $q\bar{q}$ loops of unquenched QCD.

B. The $\Delta m \ll \Gamma$ problem

Consider two resonances which are separated by a mass gap δm in the narrow resonance approximation. In general we would expect that departures from the narrow resonance approximation, which produce resonance widths Γ , ought also to produce mass shifts Δm of order Γ . Yet even though a typical hadronic mass spectrum is characterized by mass gaps δm of order 500 MeV, and typical hadronic widths are of order 250 MeV, this does not seem to happen.

We have proposed a simple resolution of this puzzle [4]. In the flux tube model of Ref. [7], the quark potential model arises from an adiabatic approximation to the gluonic degrees of freedom embodied in the flux tube. For example, the standard heavy $Q\bar{Q}$ quarkonium potential $V_{Q\bar{Q}}(r)$ is the ground state energy $E_0(r)$ of the gluonic degrees of freedom in the presence of the $Q\bar{Q}$ sources at separation r . At short distances where perturbation theory applies, the effect of N_f types of light $q\bar{q}$ pairs is (in lowest order) to shift the coefficient of the Coulombic potential from $\alpha_s^{(0)}(Q^2) = 12\pi/[33\ln(Q^2/\Lambda_0^2)]$ to

$$\alpha_s^{(N_f)}(Q^2) = \frac{12\pi}{(33 - 2N_f)\ln(Q^2/\Lambda_{N_f}^2)}.$$

The net effect of such pairs is thus to produce a *new* effective short distance $Q\bar{Q}$ potential.

Similarly, when pairs bubble up in the flux tube (i.e., when the flux tube breaks to create a $Q\bar{q}$ plus $q\bar{Q}$ system and

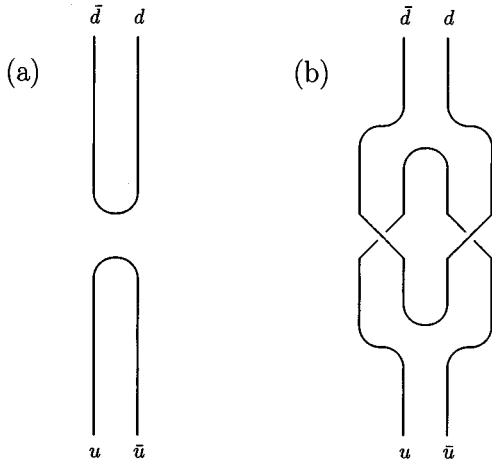


FIG. 1. (a) OZI-violation in a meson propagator by “pure annihilation,” corresponding to a disconnected double-hairpin diagram. (b) A different time ordering of the same Feynman graph gives an OZI-violating loop diagram via two OZI-allowed amplitudes.

then “heals” back to $Q\bar{Q}$), their net effect is to cause a shift $\Delta E_{N_f}(r)$ in the ground state gluonic energy which in turn produces a new long-range effective $Q\bar{Q}$ potential [8].

In Ref. [4] we showed that the net long-distance effect of the bubbles is to create a new string tension b_{N_f} (i.e., that the potential remains linear). Since this string tension is to be associated with the observed string tension, after renormalization *pair creation has no effect on the long-distance structure of the quark model in the adiabatic approximation*. Thus the net effect of mass shifts from pair creation is much smaller than one would naively expect from the typical width Γ : such shifts can only arise from nonadiabatic effects. For heavy quarkonium, these shifts can in turn be associated with states which are strongly coupled to nearby thresholds.

We should emphasize that it was necessary to sum over very large towers of $Q\bar{q}$ plus $q\bar{Q}$ intermediate states to see that the spectrum was only weakly perturbed (after unquenching and renormalization). In particular, we found that no simple truncation of the set of meson loops that can reproduce such results.

C. The survival of the OZI rule

The Introduction illustrates, via the example of ω - ϕ mixing through a $K\bar{K}$ loop, why unquenching the quark model endangers the naive quark model’s agreement with the OZI rule. In [5] we showed how this disaster is naturally averted in the flux tube model through a “miraculous” set of cancellations between mesonic loop diagrams consisting of apparently unrelated sets of mesons (e.g., the $K\bar{K}$, $K\bar{K}^* + K^*\bar{K}$, and $K^*\bar{K}^*$ loops tend to strongly cancel against loops containing a K or K^* plus one of the four strange mesons of the $L=1$ meson nonets).

Of course the “miracle” occurs for a good reason. In the flux tube model, where pair creation occurs in the 3P_0 state, the overlapping double-hairpin graphs which correspond to OZI-violating loop diagrams (see Fig. 1), cannot contribute in a closure-plus-spectator approximation since the 0^{++} quantum numbers of the produced (or annihilated) pair do

not match those of the initial and final state for any established nonet. Reference [5] demonstrates that this approximation gives zero OZI violation in all but the (still obscure) 0^{++} nonet, and shows that corrections to the closure-plus-spectator approximation are small, so that the observed hierarchy $A_{\text{OZI}} \ll \Gamma$ is reproduced.

We emphasize once again that such cancellations require the summation of a very large set of meson loop diagrams with cancellations between apparently unrelated sets of intermediate states.

D. Some comments

We believe the preceding discussion strongly suggests that models which have not addressed the effects of unquenching on spectroscopy and the OZI rule should be viewed very skeptically as models of the effects of the $q\bar{q}$ sea on hadron structure: we have shown that large towers of mesonic loops are required to understand how quarkonium spectroscopy and the OZI rule survive once strong pair creation is turned on. In particular, while pion and kaon loops (which tend to break the closure approximation due to their exceptional masses) have a special role to play, they cannot be expected to provide a reliable guide to the physics of $q\bar{q}$ pairs.

III. STRANGE QUARKS AND THE SPIN CRISIS: SOME HISTORY

Beginning in 1988 with the European Muon Collaboration (EMC) experiment [9], and continuing through a recent series of closely related experiments [10], the helicity structure functions of quarks in the proton and neutron have been measured via polarized deep inelastic scattering. When combined with measurements of axial charges in hyperon β decay and the assumption of SU(3) symmetry, these experiments indicate a “spin crisis”: only about a third of the nucleon’s helicity resides on its quarks, and about $-10 \pm 3\%$ of this helicity is lost to strange quarks [11], in violation of the Ellis-Jaffe extension [12] of the fundamental Bjorken sum rule [13].

Although generally accepted, there has been some discussion about the reliability of these conclusions. While support for them has come from other types of experiments [14], they have been criticized from other quarters for depending on an extrapolation of the structure functions to small x [15] and on a SU(3)-symmetry-based analysis of hyperon beta decay [16]. At a deeper level, reanalyses of the theoretical connection between spin-dependent deep inelastic scattering and the spin structure functions showed that the SU(3) singlet structure functions are entangled with the gluon spin structure functions via the U(1) axial anomaly [17]. This observation has led to attempts to avert the “spin crisis” by invoking a large gluonic contribution via the anomaly. This possibility should be checked by direct measurements on the glue.

The naive nonrelativistic quark model predicts that 100% of the nucleon’s helicity resides on the quarks, but, as already mentioned above, lower components of the quark spinors arising from relativistic effects are believed to lower this fraction to about 75% [6]. At the opposite extreme are naive Skyrminion models [18] which predict that the net quark

spin of the nucleons should be zero (a result which seemed supported by the initial experimental results).

If there is a large strange quark contribution to the nucleon spin, then one would also naturally expect strange contributions to nucleon magnetic and electric form factors. Purely electromagnetic scattering can only measure the four linear combinations

$$G_{M,E}^{\gamma p} = \frac{2}{3}G_{M,E}^{(u)} - \frac{1}{3}G_{M,E}^{(d)} - \frac{1}{3}G_{M,E}^{(s)}, \quad (1)$$

$$G_{M,E}^{\gamma n} = \frac{2}{3}G_{M,E}^{(d)} - \frac{1}{3}G_{M,E}^{(u)} - \frac{1}{3}G_{M,E}^{(s)}, \quad (2)$$

where $G_{M,E}^{(f)}$ is the magnetic (M) or electric (E) form factor of the quark flavor f in the proton. From parity-violating scattering on the proton one can measure two more linear combinations

$$G_{M,E}^{Zp} = \left(\frac{1}{4} - \frac{2}{3}\sin^2\theta_W \right) G_{M,E}^{(u)} + \left(-\frac{1}{4} + \frac{1}{3}\sin^2\theta_W \right) \times [G_{M,E}^{(d)} + G_{M,E}^{(s)}] \quad (3)$$

and thereby separate out the six elementary form factors $G_{M,E}^{(f)}$ for $f=u, d, \text{ and } s$. Experiments are currently underway and others are planned to measure these form factors. Such measurements appear to be the next step in understanding the physics of the spin crisis.

In the wake of the spin crisis have come a number of attempts to find theoretical descriptions less extreme than the naive quark and Skyrmion models. In 1989, Jaffe [19] pointed out that the pole fit of Höhler *et al.* to the nucleon's isoscalar electromagnetic form factors [20] could suggest the presence of significant strange currents in the nucleon. By identifying the two lightest fitted poles with the physical ω and ϕ mesons, he estimated $R_s^2 = 0.14 \pm 0.07 \text{ fm}^2$ for the strangeness radius and $\mu_s = -(0.31 \pm 0.09)\mu_N$ for the strange magnetic moment of the nucleon. (Note that Jaffe uses a sign convention in which the strange quark has positive strangeness, opposite to the Particle Data Group convention [21]. As a result, both R_s^2 and μ_s must be multiplied by $-\frac{1}{3}$ to obtain the contributions of the strange quarks to the electric and magnetic form factors of the proton. Thus, for example, a positive value for R_s^2 indicates that s quarks are farther on average from the proton's center than \bar{s} quarks. Jaffe's convention appears to have been adopted by subsequent authors, and we too shall adhere to it.)

Jaffe and Lipkin [22], building on earlier work by Lipkin [23], constructed an extended quark model in which the valence qqq component of octet baryons was supplemented with a "sea" consisting of a single $q\bar{q}$ state which was allowed to have either 0^{++} or 1^{++} quantum numbers. Their model was not predictive; it was intended only as an example of a simple extension to the quark model which could accommodate the EMC results as well as baryon magnetic moments and hyperon β decay. They found that the data could be fit with either a $(u\bar{u} + d\bar{d} + s\bar{s})$ or $(u\bar{u} + d\bar{d})$ flavor structure to the sea, though in both cases a large suppression of the purely valence component of the baryon wave functions was required. For other early analyses along these lines, see Refs. [24].

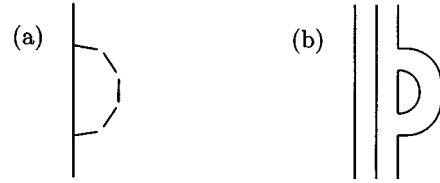


FIG. 2. A meson loop correction to a baryon propagator, drawn at (a) the hadronic level and (b) the quark level.

The renormalization of axial couplings g_A (and therefore of the fraction of the proton spin Δq carried by the quarks of flavor q) by $q\bar{q}$ pairs in the form of meson loops is a subject with a history dating back to the birth of meson exchange theories of the strong interaction. For some modern studies in the context of chiral perturbation theory, see Ref. [25]. Many recent studies, including ours, are extensions of this classic meson loop approach [26].

A model-dependent study of the $s\bar{s}$ sea based on hyperon-kaon loop diagrams was made by Koepf *et al.* in Ref. [27]. These authors used both a nonrelativistic quark model and the cloudy bag model to calculate the strangeness content of the proton arising from ΛK , ΣK , and $\Sigma^* K$ loops. After tuning the baryon-baryon-meson form factors to reproduce the nonstrange nucleon moments, they found that both models predict rather small strange moments: $\Delta s \approx -0.003$, $R_s^2 \approx -0.01 \text{ fm}^2$, and $\mu_s \approx -0.03\mu_N$.

Subsequently, Musolf and Burkhardt [28] examined the ΛK loop graph in a calculation which took its vertex form factors from the Bonn potential for baryon-baryon scattering [30], and which included seagull graphs in order to satisfy the vector current Ward-Takahashi identity. The results obtained by these authors, $\Delta s \approx -0.044$, $R_s^2 \approx -0.03 \text{ fm}^2$, and $\mu_s \approx -0.35\mu_N$, are significantly larger than those found in [27]. The discrepancy is due, at least in part, to the non-gauge invariance of the earlier calculation.

More extensive, but from our perspective still incomplete, meson loop calculations have been presented in Refs. [31]. These authors extend loop calculations to include the entire set of ground state octet pseudoscalar and vector mesons plus the ground state octet and decuplet baryons. They obtain $\Delta s \approx +0.02$. Another tack has been taken by Ito [29], who calculates the effects of kaon loops on a constituent quark, obtaining $R_s^2 \approx -0.02 \text{ fm}^2$ and $\mu_s \approx -0.12\mu_N$.

The loop and pole pictures were combined in the model of Cohen *et al.* [32], who obtained $R_s^2 \approx -0.042 \text{ fm}^2$ and $\mu_s \approx -0.28\mu_N$. These authors also calculated the strange form factors at nonzero momentum transfer.

For some reviews and for alternative models and points of view, in particular Skyrme-based calculations, see Refs. [33].

IV. A PAIR CREATION MODEL FOR THE STRANGENESS CONTENT OF THE PROTON

Our discussion of the strangeness content of the proton will be based on the quark-level process shown in Fig. 2(b). The main new feature of our calculation is that we shall sum over a *complete set* of strange intermediate states, rather than just a few low-lying states. Not only does this have a significant impact on the numerical results for Δs , R_s^2 , and μ_s ,

but, as explained above, it is *necessary* for consistency with the OZI rule and the success of quark model spectroscopy.

The lower vertex in Fig. 2(b) arises when $q\bar{q}$ pair creation perturbs the initial nucleon state vector so that, to leading order in pair creation,

$$|p\rangle \rightarrow |p\rangle + \sum_{Y^*K^*/S} \int q^2 dq |Y^*K^*q\ell S\rangle \times \frac{\langle Y^*K^*q\ell S | h_{q\bar{q}} | p \rangle}{M_p - E_{Y^*} - E_{K^*}}, \quad (4)$$

where $h_{q\bar{q}}$ is a quark pair creation operator, Y^* (K^*) is the intermediate baryon (meson), q and ℓ are the relative radial momentum and orbital angular momentum of Y^* and K^* , and S is the sum of their spins. Of particular interest is the $s\bar{s}$ pair creation by the pair creation operator $h_{s\bar{s}}$, which will generate nonzero expectation values for strangeness observables:

$$\begin{aligned} \langle O_s \rangle &= \sum_{\substack{Y^*K^*/S \\ Y'^*K'^*/S'}} \int q^2 dq q'^2 dq' \frac{\langle p | h_{s\bar{s}} | Y'^*K'^*q'\ell'S' \rangle}{M_p - E_{Y'^*} - E_{K'^*}} \\ &\times \langle Y'^*K'^*q'\ell'S' | O_s | Y^*K^*q\ell S \rangle \\ &\times \frac{\langle Y^*K^*q\ell S | h_{s\bar{s}} | p \rangle}{M_p - E_{Y^*} - E_{K^*}}. \end{aligned} \quad (5)$$

The derivation of this simple equation, including the demonstration that it is gauge invariant, is given in the Appendix. We will be considering the cases $O_s = \Delta s$, R_s^2 , and μ_s . The value of Δs can be associated (via small scale-dependent QCD radiative corrections) with the contribution of strange quarks to the deep inelastic spin-dependent structure functions and to the strange quark axial current matrix elements in the proton.

To calculate the $p \rightarrow Y^*K^*$ vertices in Eq. (4), we employ the same flux-tube-breaking model used in our earlier work. This model, which reduces to the well-known 3P_0 decay model in a well-defined limit, had its origin in applications to decays of mesons [34,35] and baryons [36]. The model assumes that a meson or baryon decays when a chromoelectric flux tube breaks, creating a constituent quark and antiquark on the newly exposed flux tube ends. The pair creation operator is taken to have 3P_0 quantum numbers:

$$h_{q\bar{q}}(t, \mathbf{x}) = \gamma_0 \left(\frac{3}{8\pi r_q^2} \right)^{3/2} \int d^3z \exp\left(-\frac{3z^2}{8r_q^2} \right) \times q^\dagger \left(t, \mathbf{x} + \frac{\mathbf{z}}{2} \right) \boldsymbol{\alpha} \cdot \nabla q \left(t, \mathbf{x} - \frac{\mathbf{z}}{2} \right). \quad (6)$$

The dimensionless constant γ_0 is the intrinsic pair creation strength, a parameter which must be fit to decay data. In our previous studies of mesons, we fit γ_0 to the $\rho \rightarrow \pi\pi$ decay width; here we find it more appropriate to fit to the $\Delta \rightarrow N\pi$ width. It turns out that the two values agree to within 20%, which is a reassuring consistency check. The operator (6) creates *constituent* quarks, hence the pair creation point is smeared out by a Gaussian factor whose width, r_q , is another parameter of the model. [In addition to being physically motivated, this smearing factor conveniently ren-

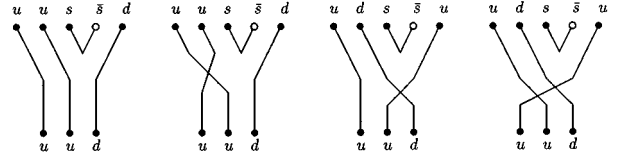


FIG. 3. Quark line diagrams for $p \rightarrow \Sigma^*K^*$ and $p \rightarrow \Lambda^*K^*$.

ders the sum in Eq. (4) finite.] As discussed in [4,5], r_q is constrained by meson decay data to be approximately 0.25 fm.

Once an $s\bar{s}$ pair is created, the decay proceeds by quark rearrangement, as shown in Fig. 3. The $p \rightarrow Y^*K^*$ decay amplitude of the first of Fig. 3 may be written as

$$\langle Y^*K^* | h_{s\bar{s}} | p \rangle = \gamma_0 \vec{\Sigma} \cdot \vec{I}, \quad (7)$$

where $\vec{\Sigma}$ is a spin overlap which can be expressed in terms of the baryon and meson spin wave functions as

$$\vec{\Sigma} \equiv \sum_{s_1 \dots s_5} \chi_{s_1 s_2 s_4}^{*Y^*} \chi_{s_3 s_5}^{*K^*} \chi_{s_1 s_2 s_3}^p \vec{\chi}_{s_4 s_5}, \quad (8)$$

with

$$\vec{\chi}_{s_4 s_5} \equiv \begin{pmatrix} 2\delta_{s_4\uparrow} \delta_{s_5\uparrow} \\ -\delta_{s_4\downarrow} \delta_{s_5\uparrow} - \delta_{s_4\uparrow} \delta_{s_5\downarrow} \\ -2\delta_{s_4\downarrow} \delta_{s_5\downarrow} \end{pmatrix}, \quad (9)$$

and \vec{I} a spatial overlap:

$$\begin{aligned} \vec{I} &= 2\gamma_0 \left(\frac{3}{4\pi b} \right)^{3/2} \int d^3k d^3p d^3s \exp\left(\frac{-s^2}{2b} \right) \\ &\times \Phi_{Y^*}^* \left[\mathbf{k}, -\sqrt{\frac{3}{2}} \left(\mathbf{p} - \frac{\mathbf{s}}{2} - \frac{m_s}{m_{uus}} \mathbf{q} \right) \right] \\ &\times \Phi_{K^*}^* \left[\mathbf{p} + \frac{\mathbf{s}}{2} - \frac{m_s}{m_{us}} \mathbf{q} \right] \mathbf{p} \exp\left(-\frac{2}{3} r_q^2 p^2 \right) \\ &\times \Phi_p \left[\mathbf{k}, -\sqrt{\frac{3}{2}} \left(\mathbf{p} + \frac{\mathbf{s}}{6} - \mathbf{q} \right) \right]. \end{aligned} \quad (10)$$

Here the Φ 's are momentum space wave functions, \mathbf{q} is the momentum of Y^* , and the m_i 's are quark masses (m_{uus} is short for $2m_u + m_s$, etc.). The factor $\exp(-s^2/2b)$ models the overlap of the initial- and final-state flux tube wave functions; its size is controlled by the physical string tension b , though our results do not depend strongly on the numerical value of b .

For the remaining quark line diagrams in Fig. 3, the decay amplitude still has the form (7), but the spin indices in Eq. (8) become permuted. [The spatial overlap in (10) remains the same thanks to the assumed symmetry of the proton's spatial wave function.]

Faced with the large number of states that contribute to the sum in Eq. (5), we have found it necessary to use simple harmonic oscillator (SHO) wave functions for the baryons and mesons in Eq. (10). The oscillator parameters β [defined by $\Phi(\mathbf{k}) \sim e^{-k^2/2\beta^2}$], were taken to be $\beta_{\text{meson}} = 0.4$ GeV for mesons (as in Ref. [35]) and $\beta_{\text{baryon}} = 0.32$ GeV for baryons (as in Ref. [37]). As discussed below, our results are quite insensitive to changes in the β 's [mainly because Eq. (5) is independent of the choice of wave functions in the closure-

limit — any complete set gives the same result — and the full calculation with energy denominators does not deviate much from this limit].

Even with SHO wave functions, the sum over intermediate states would be very difficult were it not for an important selection rule: inspection of the quark line diagrams in Fig. 3 shows that the relative coordinate of the nonstrange quarks in baryon Y^*K^* is always in its ground state. Only the relative coordinate between the strange and nonstrange quarks (i.e., the λ_{Y^*} oscillator) can become excited. This drastically reduces the number of states that must be summed over. Unfortunately, this simplification does not apply for $u\bar{u}$ or $d\bar{d}$ pair creation; we therefore postpone to a later paper the computation of their contributions to the nucleons' spin, charge radii, and magnetic moments.

We will find it useful at times to refer to the closure-spectator limit of Eq. (5). This is the limit in which the energy denominators do not depend strongly on the quantum numbers of Y^* and K^* , so that the sums over intermediate states collapse to 1, giving

$$\langle O_s \rangle \propto \langle p | h_{s\bar{s}} O_s h_{s\bar{s}} | p \rangle \propto \langle 0 | h_{s\bar{s}} O_s h_{s\bar{s}} | 0 \rangle, \quad (11)$$

where the second step follows since $h_{s\bar{s}}$ does not couple to the motion of the valence spectator quarks. We see that the expectation value of O_s is taken between the 3P_0 states created by $h_{s\bar{s}}$. From the properties of the 3P_0 wave function it then follows that $\Delta_s = R_s^2 = \mu_s = 0$ in the closure-spectator limit (a result which would not be seen if only the lowest term, or lowest few terms, were included in the closure sum).

In the next section we will present our results for the expectation values defined by Eq. (5) for the quantities Δ_s , R_s^2 , and μ_s . We will see that delicate cancellations lead to small values for these observables even though the probability of $s\bar{s}$ pairs in the proton is of order unity.

V. RESULTS

A. Strange spin content

Δ_s , the fraction of the proton's spin carried by strange quarks, is given by twice the expectation value of the s and \bar{s} spins:

$$\Delta_s = 2\langle S_z^{(s)} + S_z^{(\bar{s})} \rangle. \quad (12)$$

Let us first examine the contribution to Δ_s from just the lowest-lying intermediate state, ΛK . The P -wave ΛK state with $J = J_z = \frac{1}{2}$ is

$$|(\Lambda K)_{P(1/2)}\rangle = \sqrt{\frac{2}{3}} |(\Lambda \downarrow K)_{m=1}\rangle - \sqrt{\frac{1}{3}} |(\Lambda \uparrow K)_{m=0}\rangle. \quad (13)$$

The \bar{s} quark in the kaon is unpolarized, while the s quark in the Λ carries all of the Λ 's spin; because of the larger coefficient multiplying the first term in Eq. (13), the ΛK intermediate state alone gives a negative contribution to Δ_s .

When we add in the $(\Lambda K^*)_{P(1/2)}$ and $(\Lambda K^*)_{P(3/2)}$ states (note that the subscripts denote the quantities $\mathcal{L}(S)$ defined previously), we have

$$\Delta_s \propto \begin{pmatrix} 1 & -\sqrt{\frac{1}{3}} & \sqrt{\frac{8}{3}} \end{pmatrix} \frac{1}{18} \begin{bmatrix} -3 & \sqrt{3} & -\sqrt{24} \\ & -1 & \sqrt{8} \\ & & 10 \end{bmatrix} \begin{pmatrix} 1 \\ -\sqrt{\frac{1}{3}} \\ \sqrt{\frac{8}{3}} \end{pmatrix} \quad (14)$$

in the closure limit. Here the matrix is just $2(S_z^{(s)} + S_z^{(\bar{s})})$ (which is of course symmetric though we only show its upper triangle), and the vectors give the relative coupling strengths of the proton to $[(\Lambda K)_{P(1/2)}, (\Lambda K^*)_{P(1/2)}, (\Lambda K^*)_{P(3/2)}]$. There are a couple of things to note here.

(1) The matrix multiplication in (14) evaluates to zero; there is no net contribution to Δ_s from the ΛK and ΛK^* states in the closure limit. There are in fact many such ‘‘sub-cancellations’’ in the closure sum for Δ_s : for each fixed set of spatial quantum numbers in the intermediate state, the sum over quark spins alone gives zero (because $\langle S_z^{(s)} \rangle = \langle S_z^{(\bar{s})} \rangle = 0$ in the 3P_0 state). That is, each SU(6) multiplet inserted into Eq. (5) separately sums to zero. Moreover, the Δ_s operator does not cause transitions between $I=0$ and $I=1$ strange baryons so that the Λ and Σ sectors are decoupled, hence they individually sum to zero.

(2) Only the diagonal term in Eq. (14) corresponding to $p \rightarrow (\Lambda K^*)_{P(3/2)} \xrightarrow{\Delta_s} (\Lambda K^*)_{P(3/2)} \rightarrow p$ gives a positive contribution to Δ_s . (We use $\xrightarrow{\Delta_s}$ here to denote the action of the Δ_s operator.) All of the other terms give negative contributions. In the full calculation with energy denominators, the negative terms are enhanced because they contain kaon (rather than K^*) masses. The full calculation gives $\Delta_s = -0.065$ from ΛK and ΛK^* states. The largest individual contribution is -0.086 , from the off-diagonal term $p \rightarrow (\Lambda K)_{P(1/2)} \xrightarrow{\Delta_s} (\Lambda K^*)_{P(3/2)} \rightarrow p$.

Proceeding to intermediate states containing Σ and Σ^* baryons, we calculate

$$2(S_z^{(s)} + S_z^{(\bar{s})}) = \frac{1}{54} \begin{bmatrix} 3 & -12\sqrt{2} & 3\sqrt{3} & -6\sqrt{6} & 0 & 0 \\ & 15 & 0 & 0 & 6\sqrt{3} & -3\sqrt{15} \\ & & -7 & -10\sqrt{2} & -4\sqrt{2} & -4\sqrt{10} \\ & & & 10 & 4 & 4\sqrt{5} \\ & & & & -2 & -2\sqrt{5} \\ & & & & & 17 \end{bmatrix} \quad (15)$$

in the basis $[(\Sigma K)_{P(1/2)}, (\Sigma^* K)_{P(3/2)}, (\Sigma K^*)_{P(1/2)}, (\Sigma K^*)_{P(3/2)}, (\Sigma^* K^*)_{P(1/2)}, (\Sigma^* K^*)_{P(3/2)}]$. The corresponding relative couplings to the proton are

$$\left[-\frac{1}{3}, -\sqrt{\frac{8}{9}}, \sqrt{\frac{25}{27}}, \sqrt{\frac{8}{27}}, \sqrt{\frac{8}{27}}, \sqrt{\frac{40}{27}} \right].$$

Again, the net Δs from these states is zero in the closure limit, but this time the insertion of energy denominators does not spoil the cancellation very much: the full calculation gives $\Delta s = -0.003$ in this sector.

P -wave hyperons and kaons contribute another -0.04 to Δs , and the net contribution from all higher states is -0.025 . Thus, the result of our calculation is $\Delta s = -0.13$, in quite good agreement with the most recent extractions from experiment, $\Delta s(\text{expt}) = -0.10 \pm 0.03$ (see, e.g., Ref. [11]). We emphasize that our parameters were fixed by spectra and decay data. Moreover, the result is quite stable to parameter changes, varying by at most ± 0.025 when r_q , b , β_{baryon} , and β_{meson} are individually varied by 30%.

For comparison with other calculations, we note that in our model the ΛK intermediate state alone contributes -0.030 to Δs , and the contribution from the ΛK , ΣK , and $\Sigma^* K$ states together is (coincidentally) also -0.030 .

It is interesting to note that Δs is driven mainly by meson, rather than baryon mass splittings: if we set $m_\Lambda = m_\Sigma = m_{\Sigma^*}$, we find that Δs decreases by only about 30%, whereas it drops by about 80% if we set $m_K = m_{K^*}$. Finally, we have also computed the charm-quark contribution to the proton spin, finding $\Delta c \approx -0.01$.

B. Strangeness radius

Figure 4 defines our variables for the quarks in an intermediate state. The (squared) distances of the s and \bar{s} quarks from the baryon-meson center of mass are

$$r_s^2 = (\mathbf{r}_4 - \mathbf{R}_{\text{c.m.}})^2 = \left[-\sqrt{6} \left(\frac{m_u}{m_{uus}} \right) \boldsymbol{\lambda}_{Y^*} + \boldsymbol{\epsilon}_{K^*} \mathbf{r} \right]^2, \quad (16)$$

$$r_{\bar{s}}^2 = (\mathbf{r}_5 - \mathbf{R}_{\text{c.m.}})^2 = \left[-\left(\frac{m_u}{m_{us}} \right) \mathbf{r}_{K^*} - \boldsymbol{\epsilon}_{Y^*} \mathbf{r} \right]^2, \quad (17)$$

where $\boldsymbol{\epsilon}_{K^*} \equiv M_{K^*} / M_{Y^* K^*}$ and $\boldsymbol{\epsilon}_{Y^*} \equiv M_{Y^*} / M_{Y^* K^*}$, while by definition

$$R_s^2 \equiv r_s^2 - r_{\bar{s}}^2 \quad (18)$$

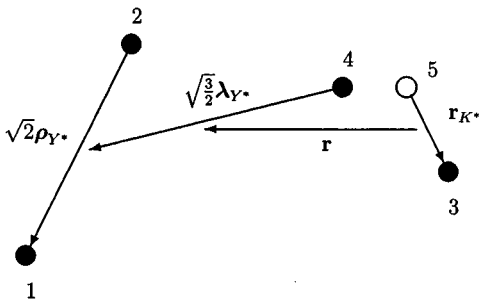


FIG. 4. Quark coordinates in an intermediate state.

is the strangeness radius.

The calculation of R_s^2 is more difficult than the calculation of Δs , for several reasons. First, the operators appearing in R_s^2 cause orbital and radial transitions among the intermediate states. Thus SHO transitions satisfying $\Delta n = 0, \pm 1$ and/or $\Delta \ell = 0, \pm 1$ are allowed, so there are many more terms to calculate (n and ℓ are orbital and radial SHO quantum numbers). Moreover, the subcancellations discussed above no longer occur, so that R_s^2 converges more slowly than Δs : we must include more states in Eq. (5) to obtain good accuracy. In addition, the basic matrix elements are more complicated: in a basis of states with good magnetic quantum numbers (m, m') we have, for example,

$$\begin{aligned} \langle n' \ell' m' | r_{K^* z} | n \ell m \rangle &= \delta_{\ell' \ell - 1} \delta_{m' m} \beta_{K^*} \\ &\times \sqrt{\frac{(\ell + m)(\ell - m)}{(2\ell + 1)(2\ell - 1)}} \\ &\times (\sqrt{n + \ell + 1/2} \delta_{n' n} \\ &- \sqrt{n + 1} \delta_{n' n + 1}) + \delta_{\ell' \ell + 1} \delta_{m' m} \beta_{K^*} \\ &\times \sqrt{\frac{(\ell + m + 1)(\ell - m + 1)}{(2\ell + 1)(2\ell + 3)}} \\ &\times (\sqrt{n + \ell + 3/2} \delta_{n' n} - \sqrt{n} \delta_{n' n - 1}) \end{aligned} \quad (19)$$

for matrix elements of the meson internal coordinate and

$$\begin{aligned} \langle q' \ell' m' | r_z | q \ell m \rangle &= i \delta_{m' m} \left\{ \delta_{\ell' \ell - 1} \sqrt{\frac{(\ell + m)(\ell - m)}{(2\ell + 1)(2\ell - 1)}} \right. \\ &\times \left[-\frac{d}{dq} + \frac{\ell - 1}{q} \right] \\ &- \delta_{\ell' \ell + 1} \sqrt{\frac{(\ell + m + 1)(\ell - m + 1)}{(2\ell + 1)(2\ell + 3)}} \\ &\times \left[\frac{d}{dq} + \frac{\ell + 2}{q} \right] \left. \right\} \frac{\delta(q - q')}{q^2} \end{aligned} \quad (20)$$

for matrix elements of the $Y^* - K^*$ relative coordinate. These matrix elements must be coupled together to give $\langle R_s^2 \rangle$ between states of definite ℓ and S with total angular momentum $\frac{1}{2}$, leading to formulas which become quite lengthy, especially for excited intermediate states. Thus we were happy to have a stringent check of our results: when we equate all of the energy denominators in Eq. (5), we must obtain the closure-spectator result, $R_s^2 = 0$.

Our results for R_s^2 are shown in Table I. With our standard parameter set, we obtain $R_s^2 = -0.04 \text{ fm}^2$. For reasonable parameter variations, R_s^2 ranges between -0.02 and -0.06 fm^2 . Table I shows that the lowest-lying SU(6) multiplets of intermediate states (i.e., the S -wave hyperons and kaons) account for about half of r_s^2 and $r_{\bar{s}}^2$. Most of the remaining contributions come from P -wave hyperons and kaons. However, R_s^2 involves a large cancellation between r_s^2 and $r_{\bar{s}}^2$, and its value does not settle down until we add in quite highly excited intermediate states. For this reason, the

TABLE I. Proton strangeness radius from hadronic loops (in fm^2). The rows give the running totals as progressively more excited intermediate states are added into the calculation. The final column thus shows the total from all intermediate states.

	Plus		Plus D waves and	All
	S waves	P waves	S wave radial excitations	states
r_s^2	0.097	0.198	0.210	0.173
$r_{\bar{s}}^2$	0.094	0.139	0.185	0.210
R_s^2	0.003	0.059	0.025	-0.04

precise numerical value (and perhaps even the sign) of R_s^2 cannot be considered definitive: our conclusion is rather that R_s^2 is small, about an order of magnitude smaller than r_s^2 and $r_{\bar{s}}^2$. This result is not too surprising: R_s^2 is exactly zero in the closure limit, and our previous hadronic loop studies [4,5] led us to expect that the full calculation with energy denominators would preserve the qualitative features of this limit.

Note that the ΛK intermediate state alone gives $R_s^2 \approx -0.01 \text{ fm}^2$ (the sign is as expected from the usual folklore) while the ΛK , ΣK , and $\Sigma^* K$ states together give -0.017 fm^2 . Nevertheless, although our sum over all states gives the same sign and order of magnitude as these truncations, Table I shows that this is just a coincidence.

C. Strange magnetic moment

The strange and antistrange quarks carry magnetic moments $-\frac{1}{3} \mu^{(s, \bar{s})}$ where

$$\mu^{(s)} = \frac{1}{2m_s} \langle 2S_z^{(s)} + L_z^{(s)} \rangle, \quad (21)$$

$$\mu^{(\bar{s})} = -\frac{1}{2m_{\bar{s}}} \langle 2S_z^{(\bar{s})} + L_z^{(\bar{s})} \rangle, \quad (22)$$

and we denote the net strange magnetic moment by μ_s :

$$\mu_s \equiv \mu^{(s)} + \mu^{(\bar{s})}. \quad (23)$$

The spin expectation values are already in hand from our Δs calculation. Referring again to Fig. 4, we see that the s and \bar{s} orbital angular momenta are given by

$$\begin{aligned} L_s &= (\mathbf{r}_4 - \mathbf{R}_{\text{c.m.}}) \times \mathbf{p}_4 \\ &= \left[-\sqrt{6} \left(\frac{m_u}{m_{uus}} \right) \boldsymbol{\lambda}_{Y^*} + \boldsymbol{\epsilon}_{K^*} \mathbf{r} \right] \times \left[-\frac{2}{\sqrt{6}} \mathbf{p}_{\lambda_{Y^*}} + \left(\frac{m_s}{m_{uus}} \right) \mathbf{q} \right], \end{aligned} \quad (24)$$

$$\begin{aligned} L_{\bar{s}} &= (\mathbf{r}_5 - \mathbf{R}_{\text{c.m.}}) \times \mathbf{p}_5 \\ &= \left[-\left(\frac{m_u}{m_{us}} \right) \mathbf{r}_{K^*} - \boldsymbol{\epsilon}_{Y^*} \mathbf{r} \right] \times \left[-\mathbf{p}_{K^*} - \left(\frac{m_s}{m_{us}} \right) \mathbf{q} \right]. \end{aligned} \quad (25)$$

Computing the expectation values of these operators presents no new difficulties beyond those encountered in the R_s^2 cal-

ulation. In fact, there are no radial transitions in this case, so there are fewer states to sum over and the sum converges more quickly.

The results obtained with our standard parameter set are

$$\langle 2S_z^{(s)} \rangle = -0.058, \quad \langle 2S_z^{(\bar{s})} \rangle = -0.074,$$

$$\langle L_z^{(s)} \rangle = 0.043, \quad \langle L_z^{(\bar{s})} \rangle = 0.038,$$

$$\mu^{(s)} = -0.025 \mu_N, \quad \mu^{(\bar{s})} = 0.060 \mu_N,$$

$$\mu_s = 0.035 \mu_N. \quad (26)$$

We predict a positive (albeit small) value for μ_s , in disagreement with the other models discussed at the beginning of this section. Where does the positive sign originate? First note that the signs of $\langle S_z^{(s)} \rangle$, $\langle L_z^{(s)} \rangle$, and $\langle L_z^{(\bar{s})} \rangle$ are correctly given by just the lowest-lying intermediate state, ΛK of Eq. (13). (We also note in passing that the L_z 's have similar magnitudes so that orbital angular momentum contributes very little to μ_s in any case.) On the other hand, the ΛK state has $\langle S_z^{(\bar{s})} \rangle = 0$, whereas we find $\langle S_z^{(\bar{s})} \rangle$ to be quite large and negative. (The main contribution comes from the off-

diagonal process $p \rightarrow (\Lambda K)_{P(1/2)} \xrightarrow{S_z^{(\bar{s})}} (\Lambda K^*)_{P(3/2)} \rightarrow p$, although there is also a significant contribution from $p \rightarrow [\Lambda(1405)K]_{S(1/2)} \xrightarrow{S_z^{(\bar{s})}} [\Lambda(1405)K^*]_{S(1/2)} \rightarrow p$.) These important terms, which drive μ_s positive, are omitted in calculations which include only kaon loops. (We find that the ΛK intermediate state alone contributes $-0.080 \mu_N$ to μ_s , and the contribution from ΛK , ΣK , and $\Sigma^* K$ together is $-0.074 \mu_N$.)

VI. CONCLUSIONS

We have presented here parameter-free calculations of the effects of the $s\bar{s}$ sea generated by strong $Y^* K^*$ loops on the low-energy, nonperturbative structure of the nucleons. These calculations represent what is to our knowledge the first such results within a framework which has been demonstrated to be consistent with the many empirical constraints which should be applied to such calculations, namely consistency with the success of the quark potential model and especially with the validity of the OZI rule.

Our results predict that observable effects from the strange sea generated by such loops arise from delicate cancellations between large contributions involving a surprisingly massive tower of virtual meson-baryon intermediate states. If correct, our conclusions rule out the utility of a search for a simple but predictive low-energy hadronic truncation of QCD. While complete (in the sense of summing over all OZI-allowed $Y^* K^*$ loops) and gauge invariant, we recall that our calculation has ignored pure OZI-forbidden effects as well as those loop diagrams directly generated by the probing current (contact terms). As a consequence, our results cannot strictly speaking be taken as predictions for Δs , R_s^2 , or μ_s . Rather, this calculation shows that a complete set of strong $Y^* K^*$ loops, computed in a model consistent with the OZI rule, gives very small observable $s\bar{s}$ effects. While such OZI-allowed processes *might* dominate,

we cannot rule out the possibility (as was also the case with $\omega - \phi$ and other meson mixing [5]) that direct OZI violation (and in this case contact graphs as well) could make additional contributions of a comparable magnitude.

The small residual effect we calculate for the loop contributions to Δs seems consistent with the most recent analyses of polarized deep inelastic scattering data. Our calculations also give small residual strange quark contributions to the charge and magnetization distributions inside the nucleons. If these contributions are dominant, it will be a challenge to devise experiments that are capable of seeing them. Indeed, they are sufficiently small that we would expect that their observation will require the development of special apparatus dedicated to this task. Given the fundamental nature of the puzzling absence of other signals for the strong $q\bar{q}$ sea in low-energy phenomena, this effort seems very worthwhile.

It would be desirable to devise tests of the mechanisms underlying the delicate cancellations which conspire to hide the effects of the sea in the picture presented here. It also seems very worthwhile to extend this calculation to $u\bar{u}$ and $d\bar{d}$ loops. Such an extension could reveal the origin of the observed violations [38] of the Gottfried sum rule [39] and also complete our understanding of the origin of the spin crisis. From our previous calculations [4], the effects of ‘‘unquenching’’ strange quarks are a good guide to the effects to be expected from up and down quarks in the absence of Pauli blocking. Since most of the created pairs are in highly excited states, Pauli blocking should be of minor importance, and so one would guess that *each* of up, down, and strange will produce a contribution to Δq of about -0.13 . When combined with the relativistic quenching of $\Delta q_{\text{valence}}$ [6], this makes it plausible to us that most of the ‘‘missing spin’’ of the proton is in orbital angular momentum.

ACKNOWLEDGMENTS

P.G. thanks Martin Savage for discussions, as well as NSERC of Canada and the U.S. Department of Energy under Grant No. DE-FG02-91ER40682 for financial support. N.I. gratefully acknowledges several helpful discussions with Michael Musolf, especially one which pointed out a potential flaw in an unpublished version of this paper.

APPENDIX: DERIVATION OF $\langle O_s \rangle$

While Eq. (5) has a simple nonrelativistic interpretation as an expectation value of O_s in the dressed state of Eq. (4), it is not obvious that it actually computes Δs , R_s^2 , and μ_s . In particular, R_s^2 and μ_s are defined in terms of charge and magnetic form factors, respectively. Here we show that the contributions to all three quantities from $s\bar{s}$ pairs arising from strong Y^*K^* loops may indeed be calculated in a *gauge invariant* fashion in our model *via* this simple formula, with each given by the usual nonrelativistic operators of Eqs. (12), (18), and (23).

We first discuss the relatively simple case of Δs , where gauge invariance plays no role. To second order in $h_{s\bar{s}}$, the graphs contributing to the nucleon matrix elements of $A_s^\mu \equiv \bar{s}\gamma^\mu\gamma_5 s$ are of two types: (1) OZI-allowed graphs where a strong $s\bar{s}$ loop has created a Y^*K^* loop and in which A_s^μ scatters the s or \bar{s} quark, and (2) pure OZI-

forbidden graphs in which A_s^μ acts on a color singlet $s\bar{s}$ state which is created and/or destroyed on the nucleon. The pure OZI-forbidden processes fall outside the scope of our model. On the other hand, OZI-allowed contributions may be calculated (with all the usual *caveats* and approximations of non-relativistic quark model calculations of axial matrix elements) according to

$$G_A^{(s)} \equiv \langle p(\mathbf{0}, +) | \bar{s}\gamma^\mu\gamma_5 s | p(\mathbf{0}, +) \rangle \quad (\text{A1})$$

$$\approx 2 \langle p(\mathbf{0}, +) | S_z^{(s)} + S_z^{(\bar{s})} | p(\mathbf{0}, +) \rangle \quad (\text{A2})$$

$$= \Delta s \quad (\text{A3})$$

as used in Sec. V A.

The discussion of R_s^2 and μ_s is considerably more involved. Our first step is to set up the Breit-frame formalism for calculating R_s^2 and μ_s . It is easily shown that the electric and magnetic form factors of the proton may be calculated *via* the formulas

$$G_E^p(q^2 = -\mathbf{Q}^2) = \frac{T_E^{\text{ext}}(\mathbf{Q})}{e\phi_E^{\text{ext}}(\mathbf{Q})}, \quad (\text{A4})$$

$$G_M^p(q^2 = -\mathbf{Q}^2) = -\frac{(2M_p/Q)T_M^{\text{ext}}(\mathbf{Q})}{ea_M^{\text{ext}}(\mathbf{Q})}, \quad (\text{A5})$$

where $T_{E,M}^{\text{ext}}(\mathbf{Q})$ are the T -matrix elements

$$T_E^{\text{ext}}(\mathbf{Q}) \equiv \left\langle p\left(+\frac{Q\hat{\mathbf{z}}}{2}, +\right) \left| \mathbf{T}_E \right| p\left(-\frac{Q\hat{\mathbf{z}}}{2}, +\right) \right\rangle, \quad (\text{A6})$$

$$T_M^{\text{ext}}(\mathbf{Q}) \equiv \left\langle p\left(+\frac{Q\hat{\mathbf{z}}}{2}, -\right) \left| \mathbf{T}_M \right| p\left(-\frac{Q\hat{\mathbf{z}}}{2}, +\right) \right\rangle, \quad (\text{A7})$$

for scattering in the external potentials

$$\phi_E^{\text{ext}}(t, \mathbf{x}) = \int d^3Q e^{i\mathbf{Q}\cdot\mathbf{x}} \phi_E^{\text{ext}}(\mathbf{Q}) \quad (\text{A8})$$

and

$$\mathbf{a}_M^{\text{ext}}(t, \mathbf{x}) = \frac{1}{2}(\hat{\mathbf{x}} - i\hat{\mathbf{y}}) \int d^3Q e^{i\mathbf{Q}\cdot\mathbf{x}} \mathbf{a}_M^{\text{ext}}(\mathbf{Q}), \quad (\text{A9})$$

respectively. [Note that all normalizations are fixed by the condition that $G_E^p(0) = 1$.]

Now consider a proton scattering off one of these external potentials subject to the additional gauge invariant perturbation created by $s\bar{s}$ pair creation. The resulting changes ΔG_E^p and ΔG_M^p are $G_E^{(s)}$ and $G_M^{(s)}$, which may therefore be associated with ΔT_E^{ext} and ΔT_M^{ext} . Thus, generically, the ΔG 's may be associated with four processes. Associated with the ‘‘naive’’ formula (5) are the two processes in which (1a) the external field probes the K^* of the Y^*K^* loop, and (1b) the external field probes the Y^* of the Y^*K^* loop. We will recall at the end of this appendix how these processes, which are of second order in the strong $s\bar{s}$ pair creation Hamiltonian density $h_{s\bar{s}}$ and third order in perturbation theory, lead to Eq. (5).

Associated with $h_{s\bar{s}}$, which has matrix elements proportional to $(-1)^{2\bar{s}}\chi_s^\dagger\sigma\chi_{-\bar{s}}(\mathbf{p}_s-\mathbf{p}_{\bar{s}})$, is a pair creation contact interaction density $h_{s\bar{s}}^{\text{contact}}$ with matrix elements proportional to $2e_s(-1)^{2\bar{s}}\chi_s^\dagger\sigma\chi_{-\bar{s}}\cdot\mathbf{A}\equiv\mathbf{j}_{s\bar{s}}^{\text{contact}}\cdot\mathbf{A}$, where $e_s=-\frac{1}{3}e$ and \mathbf{A} is the vector potential. Through this contact interaction two more processes can occur: (2a) the external field directly creates the $s\bar{s}$ pair through $h_{s\bar{s}}^{\text{contact}}$, converting the proton at momentum $-Q\hat{\mathbf{z}}/2$ into a Y^*K^* system at momentum $+Q\hat{\mathbf{z}}/2$, and then $h_{s\bar{s}}$ annihilates the $s\bar{s}$ pair, returning the Y^*K^* system to a proton at the same momentum $+Q\hat{\mathbf{z}}/2$, and (2b) $h_{s\bar{s}}$ converts the proton at momentum $-Q\hat{\mathbf{z}}/2$ into a Y^*K^* system at the same momentum, and then $h_{s\bar{s}}^{\text{contact}}$ annihilates the $s\bar{s}$ pair, turning the Y^*K^* system at momentum $-Q\hat{\mathbf{z}}/2$ to a proton at momentum $+Q\hat{\mathbf{z}}/2$.

We begin by showing that the contact terms (2a) and (2b) are not required to make the loop contributions (1a) and (1b) to R_s^2 or μ_s gauge invariant.

The case of R_s^2 is trivial: $h_{s\bar{s}}^{\text{contact}}$ is independent of $\phi_E^{\text{ext}}(t,\mathbf{x})$ in our model, so contact processes do not contribute to it.

In contrast, μ_s is determined by scattering in $\mathbf{A}_M^{\text{ext}}(t,\mathbf{x})$, which does couple to $h_{s\bar{s}}^{\text{contact}}$. From ordinary second-order time-ordered perturbation theory,

$$\frac{2T_M^{\text{ext}}(\mathbf{Q})}{e a_M^{\text{ext}}(\mathbf{Q})} = \int dq q^2 \sum_{\ell S} \frac{1}{\Delta(Q^2)} \left\langle p\left(+\frac{Q\hat{\mathbf{z}}}{2}, -\right) \times \left[t_{sc}^{q/S} + t_{cs}^{q/S} \right] p\left(-\frac{Q\hat{\mathbf{z}}}{2}, +\right) \right\rangle, \quad (\text{A10})$$

where $\Delta(Q^2)$ is an energy denominator which can easily be shown to be even in Q , and where

$$t_{sc}^{q/S} = h_{s\bar{s}}(0, \mathbf{0}) \left[[Y^*K^*]_{q/S} \left(+\frac{Q\hat{\mathbf{z}}}{2}, - \right) \right] \times \left\langle [Y^*K^*]_{q/S} \left(+\frac{Q\hat{\mathbf{z}}}{2}, - \right) \right| \mathbf{j}_{s\bar{s}}^{\text{contact}}(0, \mathbf{0})_- \quad (\text{A11})$$

and

$$t_{cs}^{q/S} = \mathbf{j}_{s\bar{s}}^{\text{contact}}(0, \mathbf{0})_- \left[[Y^*K^*]_{q/S} \left(-\frac{Q\hat{\mathbf{z}}}{2}, + \right) \right] \times \left\langle [Y^*K^*]_{q/S} \left(-\frac{Q\hat{\mathbf{z}}}{2}, + \right) \right| h_{s\bar{s}}(0, \mathbf{0}), \quad (\text{A12})$$

where $[Y^*K^*]_{q/S}(\pm Q\hat{\mathbf{z}}/2, m_{Y^*K^*})$ denotes a state with internal radial momentum q , internal orbital angular momentum ℓ and total internal spin S coupled to total angular momentum and parity $J^P = \frac{1}{2}^+$ (so that $h_{s\bar{s}}$ can connect it to the proton), with momentum $\pm Q\hat{\mathbf{z}}/2$, and with z component of spin $m_{Y^*K^*}$. Now consider the general matrix element

$$\left\langle [Y^*K^*]_{q/S} \left(+\frac{Q\hat{\mathbf{z}}}{2}, m_{Y^*K^*} \right) \right| h_{s\bar{s}}(0, \mathbf{0}) \left| p \left(-\frac{Q\hat{\mathbf{z}}}{2}, m_p \right) \right\rangle = g_{Y^*K^*p}^{q/S} (Q^2) \chi_{Y^*K^*}^\dagger \chi_p. \quad (\text{A13})$$

Since $h_{s\bar{s}}$ is a scalar operator, the form of the right-hand side of this equation is uniquely determined. In particular, it follows from parity conservation that this matrix element has no spin-flip component and therefore that when made gauge invariant *via* contact interactions, it will not generate one. We conclude that also no contributions to μ_s from contact terms are required to make the contributions of the strong Y^*K^* loops gauge invariant.

There is, of course, no reason why the underlying $s\bar{s}$ pair creation dynamics might not generate independent gauge invariant contact currents of the form $\chi_{Y^*K^*}^\dagger \epsilon^{ijk} \sigma^j Q^k \chi_p$ which *could* contribute to μ_s . Although they lie outside our goal of providing a complete calculation of the effects of $s\bar{s}$ pairs generated by strong Y^*K^* loops, it would be interesting to know the size of such effects. (We note in passing that, as a class of diagrams, they will also be subject to strong cancellations since, for example, 3S_1 pair creation followed by 3P_0 annihilation will vanish in the closure-spectator approximation.)

To complete our demonstration that Eq. (5) is the correct gauge invariant formula for the contributions of $s\bar{s}$ pairs from strong Y^*K^* loops to Δs , R_s^2 , and μ_s , we briefly recall how the third-order processes (1a) and (1b) lead to it. The analysis is very straightforward, giving

$$T_M^{\text{ext}}(\mathbf{Q})_{(1a)+(1b)} = T_M^{\text{ext}}(\mathbf{Q})_{Y^*} + T_M^{\text{ext}}(\mathbf{Q})_{K^*} \quad (\text{A14})$$

corresponding to scattering from intermediate particles Y^* and K^* , respectively, with, for example,

$$T_M^{\text{ext}}(\mathbf{Q})_{K^*} = e j_M^{K^*}(Q) a_M^{\text{ext}}(\mathbf{Q}) \sum_{m_{Y^*} m_{K^*}} \int d^3\pi \Phi_{m_{Y^*} m_{K^*}, -}^{S*}(\boldsymbol{\pi}) \times \Phi_{m_{Y^*} m_{K^*}, +}^{S*}(\boldsymbol{\pi} + \epsilon_{Y^*} \mathbf{Q}) \quad (\text{A15})$$

$$= e j_M^{K^*}(Q) a_M^{\text{ext}}(\mathbf{Q}) \sum_{m_{Y^*} m_{K^*}} \int d^3r \psi_{m_{Y^*} m_{K^*}, -}^{S*}(\mathbf{r}) \times e^{-i\mathbf{Q}\cdot\mathbf{r}} \psi_{m_{Y^*} m_{K^*}, +}^{S*}(\mathbf{r}), \quad (\text{A16})$$

where $\mathbf{r}_{K^*} = \epsilon_{Y^*} \mathbf{r}$ and where

$$\Phi_{m_{Y^*} m_{K^*}, s}^{S*}(\boldsymbol{\pi}) = \langle [Y^*(\epsilon_{Y^*} \mathbf{P} + \boldsymbol{\pi}, m_{Y^*}) K^*(\epsilon_{K^*} \mathbf{P} - \boldsymbol{\pi}, m_{K^*})]_{\ell S} | h_{s\bar{s}}(0, \mathbf{0}) | p(\mathbf{P}, s) \rangle \quad (\text{A17})$$

is the internal relative momentum wave function of Y^* and K^* ‘‘inside’’ the proton [which is independent of the (small) total momentum \mathbf{P}], and ψ is its Fourier transform. Clearly an exactly analogous formula appears for $T_M^{\text{ext}}(\mathbf{Q})_{Y^*}$ and the two, having as they do simple constituent interpretations, lead to the ‘‘naive’’ Eq. (5).

- [1] G. 't Hooft, Nucl. Phys. **B72**, 461 (1974); E. Witten, *ibid.* **B160**, 57 (1979). For some recent very important developments in the $1/N_c$ expansion for baryons, see R. Dashen and A. Manohar, Phys. Lett. B **315**, 425 (1993); **315**, 438 (1993); R. Dashen, E. Jenkins, and A. Manohar, Phys. Rev. D **49**, 4713 (1994); **51**, 2489 (1995).
- [2] S. Okubo, Phys. Lett. **5**, 165 (1963); Phys. Rev. D **16**, 2336 (1977); G. Zweig, CERN Report No. 8419 TH 412, 1964 (unpublished); reprinted in *Developments in the Quark Theory of Hadrons*, edited by D. B. Lichtenberg and S. P. Rosen (Hadronic Press, Massachusetts, 1980); J. Iizuka, K. Okada, and O. Shito, Prog. Theor. Phys. **35**, 1061 (1966); J. Iizuka, Prog. Theor. Phys. Suppl. **37-38**, 21 (1966).
- [3] H.J. Lipkin, Nucl. Phys. **B291**, 720 (1987); Phys. Lett. B **179**, 278 (1986); Nucl. Phys. **B244**, 147 (1984); Phys. Lett. **124B**, 509 (1983).
- [4] P. Geiger and N. Isgur, Phys. Rev. D **41**, 1595 (1990).
- [5] P. Geiger and N. Isgur, Phys. Rev. D **44**, 799 (1991); Phys. Rev. Lett. **67**, 1066 (1991); Phys. Rev. D **47**, 5050 (1993); P. Geiger, *ibid.* **49**, 6003 (1993).
- [6] N.N. Bogoliubov, Ann. Inst. Henri Poincaré **8**, 163 (1968); A. Le Yaouanc *et al.*, Phys. Rev. D **9**, 2636 (1974); **15**, 844 (1977), and references therein; Michael J. Ruiz, *ibid.* **12**, 2922 (1975); A. Chodos, R.L. Jaffe, K. Johnson, and C.B. Thorn, *ibid.* **10**, 2599 (1974).
- [7] N. Isgur and J. Paton, Phys. Rev. D **31**, 2910 (1985).
- [8] Unlike the Coulombic region where the $q\bar{q}$ pairs are all virtual, in the long-distance region pair production can also lead to real dissociation into a $Q\bar{q}$ plus $q\bar{Q}$ system if the energy $E_0(r)$ corresponds exactly to the sum of the masses of states of these two meson subsystems. In the language of adiabatic surfaces, these dissociations occur when the $Q\bar{Q}$ adiabatic surface unperturbed by $q\bar{q}$ pair creation crosses the energies $E_{ij} = m_i^{Q\bar{q}} + m_j^{q\bar{Q}}$ corresponding to the two-meson adiabatic surfaces (which are independent of r for large r and have no continuum parts since the Q and \bar{Q} are fixed). The shifted adiabatic surface can, of course, be tracked through the level crossings to follow the quantum state that remains dominantly a $Q\bar{Q}$ pair connected by a flux tube.
- [9] EM Collaboration, J. Ashman *et al.*, Phys. Lett. B **206**, 364 (1988); Nucl. Phys. **B328**, 1 (1989).
- [10] SM Collaboration, B. Adeva *et al.*, Phys. Lett. B **302**, 533 (1993); E142 Collaboration, P.L. Anthony *et al.*, Phys. Rev. Lett. **71**, 959 (1993); SM Collaboration, D. Adams *et al.*, Phys. Lett. B **329**, 399 (1994); E143 Collaboration, K. Abe *et al.*, Phys. Rev. Lett. **74**, 346 (1995).
- [11] J. Ellis and M. Karliner, Phys. Lett. B **341**, 397 (1995).
- [12] J. Ellis and R.L. Jaffe, Phys. Rev. D **9**, 1444 (1974); **10**, 1669 (1974).
- [13] J.D. Bjorken, Phys. Rev. **148**, 1467 (1966); Phys. Rev. D **1**, 1376 (1970).
- [14] L.A. Ahrens *et al.*, Phys. Rev. D **35**, 785 (1987).
- [15] F.E. Close and R.G. Roberts, Phys. Rev. Lett. **60**, 1471 (1988).
- [16] H.J. Lipkin, Phys. Lett. B **214**, 429 (1988).
- [17] G. Altarelli and G.G. Ross, Phys. Lett. B **212**, 391 (1988); R.D. Carlitz, J.C. Collins, and A.H. Mueller, *ibid.* **214**, 229 (1988); D.B. Kaplan and A. Manohar, Nucl. Phys. **B310**, 527 (1988); R.L. Jaffe, Phys. Lett. B **193**, 101 (1987); R.L. Jaffe and A. Manohar, Nucl. Phys. **B337**, 509 (1990); R.L. Jaffe, Nucl. Phys. **A547**, 17c (1992).
- [18] S.J. Brodsky, J. Ellis, and M. Karliner, Phys. Lett. B **206**, 309 (1988); J. Ellis and M. Karliner, *ibid.*, **B213**, 73 (1988).
- [19] R.L. Jaffe, Phys. Lett. B **229**, 275 (1989).
- [20] G. Höhler *et al.*, Nucl. Phys. **B114**, 505 (1976).
- [21] Particle Data Group, L. Montanet *et al.*, Phys. Rev. D **50**, 1173 (1994).
- [22] R.L. Jaffe and H.J. Lipkin, Phys. Lett. B **266**, 458 (1991).
- [23] H.J. Lipkin, Phys. Lett. B **256**, 284 (1991).
- [24] G.P. Ramsey, J.-W. Qiu, D. Richards, and D. Sivers, Phys. Rev. D **39**, 361 (1989); C.E. Carlson and J. Milana, *ibid.* **40**, 3122 (1989).
- [25] E. Jenkins and A.V. Manohar, Phys. Lett. B **255**, 558 (1991); **259**, 353 (1991).
- [26] For some background, see J.D. Bjorken and S.D. Drell, *Relativistic Quantum Mechanics* (McGraw-Hill, New York, 1964). The classic loop approach has more recently been incorporated into bag and constituent quark models: see, e.g., G.E. Brown and M. Rho, Phys. Lett. **82B**, 177 (1977); S. Thèberge, A.W. Thomas, and G.A. Miller, Phys. Rev. D **22**, 2838 (1980); Y. Nogami and N. Ohtsuka, *ibid.* **26**, 261 (1982).
- [27] W. Koepf, E.M. Henley, and S.J. Pollock, Phys. Lett. B **288**, 11 (1992).
- [28] M.J. Musolf and M. Burkardt, Z. Phys. C **61**, 433 (1994).
- [29] H. Ito, Phys. Rev. C **52**, R1750 (1995).
- [30] B. Holzenkamp, K. Holinde, and J. Speth, Nucl. Phys. **A500**, 485 (1989).
- [31] A. Szczurek and H. Holtmann, Acta Phys. Pol. B **24**, 1833 (1993); H. Holtmann, A. Szczurek, and J. Speth, Nucl. Phys. **A596**, 631 (1996).
- [32] T.D. Cohen, H. Forkel, and M. Nielsen, Phys. Lett. B **316**, 1 (1993); H. Forkel *et al.*, Phys. Rev. C **50**, 3108 (1994).
- [33] B.R. Holstein, in *Proceedings of the Caltech Workshop on Parity Violation in Electron Scattering*, edited by E.J. Beise and R.D. McKeown (World Scientific, City, 1990), p. 27; G. Karl, Phys. Rev. D **45**, 247 (1992); M. Burkhardt and B.J. Warr, *ibid.* **45**, 958 (1992); J. Ellis and M. Karliner, in *PANIC XIII: Particles and Nuclei*, Proceedings of the 13th International Conference, Perugia, Italy, 1993, edited by A. Pascolini (World Scientific, Singapore, 1994), p. 48, Report No. hep-ph/9310272 (unpublished); N.W. Park, J. Schechter, and H. Weigel, Phys. Rev. D **43**, 869 (1991); N.W. Park and H. Weigel, Nucl. Phys. **A541**, 453 (1992); J. Keppler and H.M. Hofmann, Phys. Rev. D **51**, 3936 (1995); M.J. Musolf *et al.*, Phys. Rev. **239**, 1 (1994); T.P. Cheng and L.-F. Li, Phys. Rev. Lett. **74**, 2872 (1995); H.-C. Kim, T. Watabe, and K. Goeke, "Update of the Stranger Story: The Strange Vector Form Factors of the Nucleon," Report No. RUB-TPII-11/95 (unpublished).
- [34] L. Micu, Nucl. Phys. **B10**, 521 (1969); A. Le Yaouanc, L. Oliver, O. Pene, and J.-C. Raynal, Phys. Rev. D **8**, 2233 (1973); Phys. Lett. **71B**, 397 (1977); **72B**, 57 (1977); W. Roberts and B. Silvestre-Brac, Few-Body Syst. Suppl. **11**, 171 (1992); P. Geiger and E.S. Swanson, Phys. Rev. D **50**, 6855 (1994).
- [35] R. Kokoski and N. Isgur, Phys. Rev. D **35**, 907 (1987).
- [36] Fl. Stancu and P. Stassart, Phys. Rev. D **38**, 233 (1988); **39**, 343 (1989); **41**, 916 (1990); **42**, 1521 (1990); S. Capstick and W. Roberts, *ibid.* **47**, 1994 (1993); **49**, 4570 (1994).
- [37] N. Isgur and G. Karl, Phys. Rev. D **20**, 1191 (1979).
- [38] New Muon Collaboration, P. Amaudruz *et al.*, Phys. Rev. Lett. **66**, 2712 (1991); M. Arneodo *et al.*, Phys. Rev. D **50**, R1 (1994); NA 51 Collaboration, A. Baldit *et al.*, Phys. Lett. B **332**, 244 (1994).

- [39] K. Gottfried, Phys. Rev. Lett. **18**, 1174 (1967). For some recent theoretical studies, see W.-Y. P. Hwang and J. Speth, Chin. J. Phys. **29**, 461 (1991); A. Szczurek and J. Speth, Nucl. Phys. **A555**, 249 (1993); V.R. Zoller, Z. Phys. C **53**, 443 (1992); S. Kumano, Phys. Rev. D **43**, 59 (1991); **43**, 3067 (1991); S. Kumano and J. Londergan, *ibid.* **44**, 717 (1991); E.M. Henley and G.A. Miller, Phys. Lett. B **251**, 453 (1990); A. Signal, A.W. Schreiber, and A.W. Thomas, Mod. Phys. Lett. A **6**, 271 (1991); W.-Y. P. Hwang, J. Speth, and G.E. Brown, Z. Phys. A **339**, 383 (1991); Holtmann, Szczurek, and Speth [31].